Antiviral Research 84 (2009) 14–22

Contents lists available at ScienceDirect

Antiviral Research

journal homepage: www.elsevier.com/locate/antiviral

Novel HCV replication mouse model using human hepatocellular carcinoma xenografts

Carl Guévin, Alain Lamarre, Patrick Labonté*

Institut National de la Recherche Scientifique-Institut Armand-Frappier (INRS-IAF), 531 blvd. Des Prairies, Laval, Québec, Canada H7 V 1B7

ARTICLE INFO

Article history:
Received 22 October 2008
Received in revised form 9 July 2009
Accepted 15 July 2009

Keywords:
HCV
Mouse model
Antiviral
JFH1

ABSTRACT

In the absence of an immunocompetent mouse model for HCV replication, we developed a convenient xenograft mouse model that produces infectious viral particles. For this purpose, HCV-permissive tumors were generated in SCID/beige mice using a tumorigenic population of the human hepatocarcinoma-derived Huh7 cell line. Following infection, HCV RNA increased in the mouse sera and the human tumor by up to 10^5 GE/ml and 10^7 GE/μg of RNA, respectively. Immunohistochemistry analysis revealed that active viral replication had taken place within the tumor. Moreover, virus recovered from infected mice sera was readily infectious in cell culture. Finally, we showed that interferon-α and the protease inhibitor BILN-2061 inhibited the cell culture HCVcc strain JFH1 replication *in vivo*. In conclusion, we developed a simple and inexpensive mouse model that allows the production of infectious HCV particles *in vivo*. Such a model will be an extremely valuable tool for the characterization of promising drug candidates.

1. Introduction

Hepatitis C virus (HCV) is a leading cause of chronic hepatitis, cirrhosis and hepatocellular carcinoma worldwide (Sarbah and Younossi, 2000). In the absence of a prophylactic vaccine or a specific antiviral agent, the best treatment currently available for HCV infection is the combination therapy of peg-interferon-α and ribavirin (Di Bisceglie et al., 2002). HCV is a positive-strand RNA enveloped virus that is classified as a *Hepacivirus* within the *Flaviviridae* family (Simmonds et al., 2005). The RNA genome is ~9.6 kb in length and produces a single polyprotein of 3010–3040 amino acids that is processed by a combination of viral and cellular proteases, giving rise to at least 10 individual proteins (Bartenschlager et al., 2004). Even thought recent work has led to the development of *in vitro* HCV infection systems, the evaluation of experimental vaccines and therapeutic agents against HCV still requires the development of animal models (Lindenbach and Rice, 2005; Wakita et al., 2005; Zhong et al., 2005). There is no convenient animal model in which to study HCV replication *in vivo*. In fact, the only known natural host for HCV is human, although chimpanzee can be infected experimentally and is still considered to be the best animal model available (Bukh, 2004; Shoukry et al., 2004; Thimme et al., 2002). However, ethical issues, limited availability, and the high cost of these primates severely limit their use. As an alternative, attempts to produce mice models have met with moderate success (Ilan et al., 2002; Kneteman et al., 2006; Labonté et al., 2002; Mercer et al., 2001). The existing mouse models are expensive and technically challenging, which limits their usefulness for drug screening as well as for the study of HCV biology. We have previously reported the generation of a murine model with which to study HCV replication based on the establishment of HCV-infected tumors in immunodeficient mice (Labonté et al., 2002). For this purpose, a highly tumorigenic Huh7 subclone (HuT7-3) was developed and was able to promote the formation of human hepatocarcinoma subcutaneously as well as orthotopically in nude mice (Labonté et al., 2000). In this model, HCV-positive human sera were used as the source of infectious particles to initiate infection in mice. Viral replication was achieved but viral titers were low, due to the poor susceptibility of the human hepatoma cells to blood-derived HCV particles. Using the cell culture HCV (HCVcc) strain JFH1 and the Huh7 cell line, this difficulty can now be overcome (Wakita et al., 2005). Recently, a xenograft mouse model with an implanted mouse-adapted luciferase replicon-containing Huh7 cell line has been described (Zhu et al., 2006). The replication level of the HCV RNA replicon in individual mice was monitored by measuring luciferase activity. However, this replicon-based mouse model does not produce HCV particles.

In this report, we describe the development and use of a simple, inexpensive and reliable mouse model that allows the production of infectious HCV particles *in vivo*. By using a genotype 2a infectious clone that replicates and produces infectious virus in cell culture, we demonstrated that the strain JFH1 can establish robust infections in SCID/beige mice harboring human hepatocarcinoma xenografts. Furthermore, we validated the model using two

* Corresponding author. Tel.: +1 450 687 5010x4331; fax: +1 450 686 5314.
E-mail address: patrick.labonte@iaf.inrs.ca (P. Labonté).

0166-3542/$ – see front matter © 2009 Elsevier B.V. All rights reserved.
doi:10.1016/j.antiviral.2009.07.009

well-known HCV inhibitors, Intron-A (IFN-α2b) and BILN-2061. This *in vivo* model of HCV infection should provide a drug discovery asset to guide the selection of anti-HCV drug candidates.

2. Materials and methods

2.1. Animals

Female C.B17 SCID (SCID), SCID/beige and CD1 nu/nu mice (5–13 weeks old) were purchased from Charles River Laboratories (Saint-Constant, Quebec, Canada) and were housed and treated as required by the Canadian Council of Animal Care.

2.2. Cell culture

Huh7, Huh7-7, HuT7-3 and HEK-293 cells were maintained in DMEM supplemented with 10% fetal calf serum and penicillin–streptomycin–glutamine (Gibco, Carlsbad, CA).

2.3. HCV RNA transcription and transfection

The HCVcc strain JFH1 was obtained from Dr Takaji Wakita, having been derived from a Japanese patient with fulminant hepatitis (Kato et al., 2001). To generate genomic JFH1, the pJFH1 plasmid was linearized at the 3′ end of the HCV cDNA by *Xba*I digestion. The linearized DNA was then purified and used as a template for *in vitro* transcription (MEGAscript; Ambion, Austin, TX). *In vitro*-transcribed HCV RNA or total cell RNA was transfected into cells using a modified electroporation protocol (Krieger et al., 2001). Briefly, trypsinized cells were washed twice with serum-free medium and resuspended to a final concentration of 1×10^7 cells/ml. Ten micrograms of HCV RNA were then mixed with 0.4 ml of the cells in a 4 mm cuvette. A Gene Pulser system (BioRad Laboratories, Hercules, CA) was used to deliver a single pulse of 0.27 kV, 100 Ω, 960 μF.

2.4. Infection with HCV JFH1

Supernatant from Huh7 cells harvested 60 days post-transfection was used to infect Huh7-7 cells (10–15% confluency) at an MOI of 0.05 in a T75 flask. Prior to subcutaneous injection of infected cells in mice, the ongoing infection was confirmed by indirect immunofluorescence. For *in vivo* infection of the tumor, intratumoral injection of 600 FFU of JFH1 virus was performed. For *in vitro* infection with mouse sera, Huh7 cells were seeded 24 h before infection at a density of 1×10^5 cells/well in a six-well plate and incubated overnight with mouse sera (10^3 HCV genome equivalent (GE)). The infection was confirmed by immunofluorescence at 3 and 15 days post-infection.

2.5. Implantation of subcutaneous xenograft

The tumorigenicity of Huh7, Huh7-7 and HuT7-3 cells was evaluated by inoculating 5×10^6 cells, resuspended in 0.2 ml of PBS, subcutaneously into the right flanks of 6–8-week female SCID/beige mice. The tumor volume and the body weight of mice were evaluated once a week. Mice were euthanized at 4 weeks post-injection or when tumor volume was >2500 mm^3. Tumors were removed and processed for RNA, proteins, histological and immunohistochemical analysis.

2.6. Adaptation of Huh7 cells to form solid tumor growth

A SCID/beige mouse harboring a (2000 mm^3) xenograft human tumor was sacrificed and the tumor was excised, dissected into 2–5 mm cubes and transplanted subcutaneously into anaesthetized SCID/beige mice. This process was repeated seven times and the resulting tumor was digested with collagenase treatment (Labonté et al., 2000) and expanded *in vitro* to create the Huh7-7 tumorigenic cell population.

2.7. Drug treatment

When tumors reached 300–500 mm^3, mice were randomly divided into three groups and injected once a day in the subcutaneous suprascapular area of the animal with IFN-α2b (Intron-A; 20,000 IU) or BILN-2061 30 mg/kg or saline solution (control). Treatments lasted 5 and 4 days for Intron-A and BILN-2061, respectively. No sign of toxicity was observed in any treated animal.

2.8. Quantitative RT-PCR

Total cellular RNA from tumor tissue samples and viral RNA from mice sera were extracted and purified with Trizol as described by the manufacturer (Invitrogen). The cDNA was prepared from 250 ng of total cellular RNA or 50 μl of sera from mice. Briefly, RNAs were incubated for 3 min at 70 °C then cooled on ice for 2 min before the addition of 4 μl of RT-buffer 5× (Invitrogen), 2 μl DTT (0.1 M), 1 μl random primer p(dN6) (100 ng/μl), 1 μl dNTP (20 mM), 20 U of RNAsin and 100 U of MMLV reverse-transcriptase. Samples were incubated for 10 min at 25 °C and 1 h at 37 °C. To inactivate the MMLV, samples were incubated for 15 min at 70 °C and the cDNA was diluted to a final volume of 200 μl with RNase-free water. The primers used for amplification were: 5′UTR-R: 5′-GAGTGGGTTTATCCAAGAAAG-3′ and 5′UTR-F: 5′-TCTGCGGAACCGGTGAGT-3′. The mixture consisted of 2.5 μl of cDNA in a final volume of 25 μl of the reaction mixture containing 8.6 μl H_2O, 0.5 μl of probe FAM-UTR (12.5 μM) CCGGAATTGCCGGGAAGACTG, and 0.25 μl (90 μM) of each HCV primer. For the internal control, the 18S ribosomal RNA Kit was used according to the manufacturer's instructions (Applied Biosystems). The mixture was completed with 12.5 μl of the Taqman Universal Master Mix 2× (Applied Biosystems) and the amplification was performed according to the manufacturer's instructions in a Rotor-Gene RG-3000 (Corbet Research).

2.9. Indirect immunofluorescence

Huh7 or Huh7-7 infected cells were seeded on a cover glass (2×10^4 cells per cover glass) and were fixed with 4% paraformaldehyde in PBS. Staining of HCV NS5A was performed using a polyclonal anti-NS5A antibody (obtained from Dr O. Nicolas, ViroChem Pharma) for 1 h (1:200). Human albumin was detected using a polyclonal anti-human albumin (Dako) (1/100). Both antibodies were used in PBS 3% BSA, 10% FBS and 10% triton X-100. Antibodies were washed four times in PBS and bound antibodies were detected by incubation for 1 h with anti-rabbit goat Alexa 488 antibody at a dilution of 1:500. Unbound antibodies were washed four times with PBS and nuclei were stained with DAPI. Immunofluorescence analysis was performed with a Nikon microscope TE2000.

2.10. Titration of infectious HCV

Titration was performed as previously described (Zhong et al., 2005). Briefly, cell supernatants or mice sera were 10-fold or 2-fold serially diluted in complete DMEM and used to infect 10^4 Huh7-5 cells in 96-well plates (Corning). The virus was incubated with cells for 3 h at 37 °C and then washed away with PBS and supplemented with fresh complete DMEM. The level of HCV infection was determined 3 days post-infection by immunofluorescence staining for HCV NS5A. The viral titer was expressed as focus-forming units

per milliliter of supernatant (FFU/ml), determined by the average number of NS5A-positive foci detected at the highest dilutions.

2.11. Histological and immunohistochemical analysis

Briefly, all tissue sections were fixed in formalin and embedded in paraffin. Sections from tumors were cut at 3–5 μm, mounted on glass, and dried overnight at 37 °C. All sections were then deparaffinized in xylene, rehydrated through a graded alcohol series, and washed in PBS. For immunohistochemistry, the sections were incubated with 0.6% H_2O_2 in normal goat serum for 20 min to block endogenous peroxidase activity (Vectastain, ABC kit, Vector Laboratories, Burlingame, CA), followed by a rabbit polyclonal anti-core 1:100 (obtained from Dr Denis Leclerc, Université Laval, Canada) or a rabbit polyclonal anti-human albumin (Dako) for 1 h at room temperature. The sections were then washed twice in PBS for 5 min each and incubated for 1 h in biotinylated anti-rabbit IgG (Vectastain, ABC kit) at room temperature. After three washes in PBS for 5 min each, the sections were incubated with the ABC complex (Vectastain, ABC kit) for 30 min at room temperature. Sections were then washed in PBS and developed with diaminobenzidine (DAB, Dako detection kit; Dako, Carpinteria, CA) for 7 min and counterstained with hematoxylin.

2.12. Western blot analysis

Cell lysates were prepared by treating tissues with ice-cold lysis buffer [20 mM Tris–HCl (pH 8), 10% NP40, 10% glycerol, 137 mM NaCl, 10 mM EDTA (pH 8), and protease inhibitor cocktail (Roche Applied Science, Mannheim, Germany)] for 20 min on ice followed by centrifugation at 4 °C for 15 min to sediment particulate materials. The protein concentration was measured using the BCA Protein Assay kit (Pierce; Rockford, IL). After SDS-PAGE electrophoresis, protein samples were transferred to an immuno-blot PVDF membrane for protein blotting (Bio-Rad) for 45 min. Non-specific binding sites were blocked for 1 h in PBS 5% skimmed milk and the membrane was stained for 1 h with the primary antibodies. The antibodies used were anti-NS5A 1:2000, anti-core 1:1000 (obtained from Dr Denis Leclerc, Laval University, Canada) and anti-E2 1:500 (mouse monoclonal, Biodesign International, Saco, ME). After incubation with the primary antibody, the membranes were washed four times in PBS 0.1% Tween-20. Bound antibodies were detected by incubation for 45 min with a goat anti-rabbit HRP antibody (1:10,000, Jackson Immunosearch) or goat anti-mouse (1:5000, Promega). The signals were developed with SuperSignal™ West Pico chemiluminescent substrate (Pierce).

2.13. Flow cytometry

Cell surface expression of TFR, CLDN-1 and CD81 was monitored by recovering the cells using Versene™ (TFR and CLDN-1) or trypsin, 0.25% EDTA (CD81) (Invitrogen). Approximately 1×10^6 cells were fixed in PBS 4% formaldehyde for 10 min and blocked in PBS 3% FBS for 30 min at 4 °C. Cells were stained for 1 h at 4 °C with anti-TFR (BD Pharmingen™), anti-CLDN-1 (Abnova) and anti-CD81 (Santa Cruz Biotechnology) antibody at 1 μg/ml in PBS 3% FBS. Cells were washed twice in PBS and incubated for 30 min at 4 °C with mouse-specific secondary antibodies conjugated with fluorescein isothiocyanate (FITC) (1:1000) (Jackson ImmunoResearch) in PBS 3% FBS, respectively. For the detection of the LDLR at the cell surface, cells were resuspended in Versene™ and treated as for the detection of CD81. The primary antibody was an anti-LDLR (C7) (Santa Cruz Biotechnology) used at 1 μg/ml and the secondary antibody was a mouse-specific secondary antibody conjugated with fluorescein isothiocyanate (1:1000) (Jackson ImmunoResearch) respectively. All samples were analyzed immediately using a FACSCalibur™.

2.14. Sucrose density gradient analysis

Supernatant from JFH1-infected Huh7, Huh7-7 cells and pooled infected mouse sera were centrifuged at 4000 rpm for 5 min to remove cellular debris. Samples (800 μl) were loaded by overlaying onto a TNE buffer (50 mM Tris–HCl, pH 8; 100 mM NaCl; 1 mM EDTA)-based 10–50% sucrose gradient followed by centrifugation at 120,000 × *g* for 16 h at 4 °C using a SW60Ti rotor in a Beckman Coulter Optima™ L-100 Ultracentrifuge. Fractions of 275 μl were collected from the bottom of the gradient. Buoyant densities were determined by refractometry on a Fisher Refractometer (Fisher Scientific). The fractions were analyzed by qRT-PCR to detect HCV RNA, and the FFU were calculated as described above.

3. Results

3.1. Development of human hepatocellular carcinoma in xenograft mouse model

We have previously reported the generation of a highly tumorigenic clone of the Huh7 cell, named HuT7-3 (Labonté et al., 2000). The HuT7-3 cells were able to establish solid white tumors either subcutaneously or in the mouse liver. However, the HuT7-3 cells were not susceptible to HCV JFH1 infection and normal Huh7 cells were used for further development of the human xenograft in mice. Indeed, subcutaneous injection of Huh7 cells has been shown to induce tumors in immunodeficient mice (Chiba et al., 2006; Esposito et al., 2006; Kito et al., 2003). In our hands, the tumorigenicity of Huh7 cells was low and resulted in 20–38% of successful xenograft implantation in immunocompromized mice (Table 1). As expected, SCID/beige mice were more susceptible to xenograft development than SCID or CD1 nu/nu mice. The initial expansion of the tumors was apparent at 2–3 weeks post-injection with tumors reaching a volume of 2000 mm^3 about 2–3 weeks after the onset of tumor growth. Interestingly, all tumors (28 out of 28) were extremely vascularized with a coloration similar to that of liver tissue (Fig. 2A). Metastases were never detected grossly or microscopically. Importantly, cells recovered from mouse tumor tissue were still susceptible to HCV JFH1 virus *in vitro* (data not shown, and Table 1).

With an unsatisfactory success rate of 20–38% using normal Huh7, we decided to improve the capability of the global Huh7 population to initiate tumor formation. We thus performed serial passages of 2–4 mm^3 tumor block from mouse to mouse. The resulting Huh7 population, named Huh7-7 (seven *ex vivo* serial passages) was very efficient at inducing tumors while retaining susceptibility to HCVcc infection *in vitro* (Table 1).

Table 1
Tumorigenicity of Huh7 in immunocompromized mice.

Cell line	Cell susceptibility to HCVcc *in vitro*	Mice strain	Number of mice with tumor	Percent of mice with tumor
HuT7-3[a]	No	CD1 nu/nu	5/5	100
Huh7[b]	Yes	CD1 nu/nu	2/10	20
		SCID	2/6	33
		SCID/beige	14/32	38
Huh7-7[c]	Yes	SCID/beige	27/30	90

[a] Colony of Huh7; highly tumorigenic (Labonté et al., 2003).
[b] Normal Huh7; low tumorigenicity.
[c] *Ex vivo*-selected subpopulation of Huh7; medium tumorigenicity.

During the selection of Huh7 populations with enhanced tumorigenicity, we observed that tumorigenic populations had a tendency to lose their susceptibility to JFH1 infection but not in the case of the Huh7-7 cells. Therefore, we decided to compare the Huh7-7 population to normal Huh7 cells. First, we analyzed the cell surface expression of key receptors for HCV infection such as CD81, claudin-1 and LDL-R as well as the transferring receptor (TFR or CD71), a well-known receptor that is involved in iron uptake in the liver (Fig. 1A). Although minor divergences were observed in the expression of TFR, CLDN-1 and LDLR, two very distinct CD81 expression profiles were observed in Huh7-7 cells. Indeed, only 75% of the cell populations expressed CD81 at a level comparable to normal Huh7 cells. The reduction in CD81 expression in the remaining 25% of the population did not seem to affect their susceptibility to JFH1 since >90% of the cells were readily infected *in vitro* and *in vivo* (Fig. 1C, right and Fig. 2A). Furthermore, no significant divergence in viral replication was observed in Huh7 and Huh7-7 cells (Fig. 1C, left) and the specific infectivity of the virus

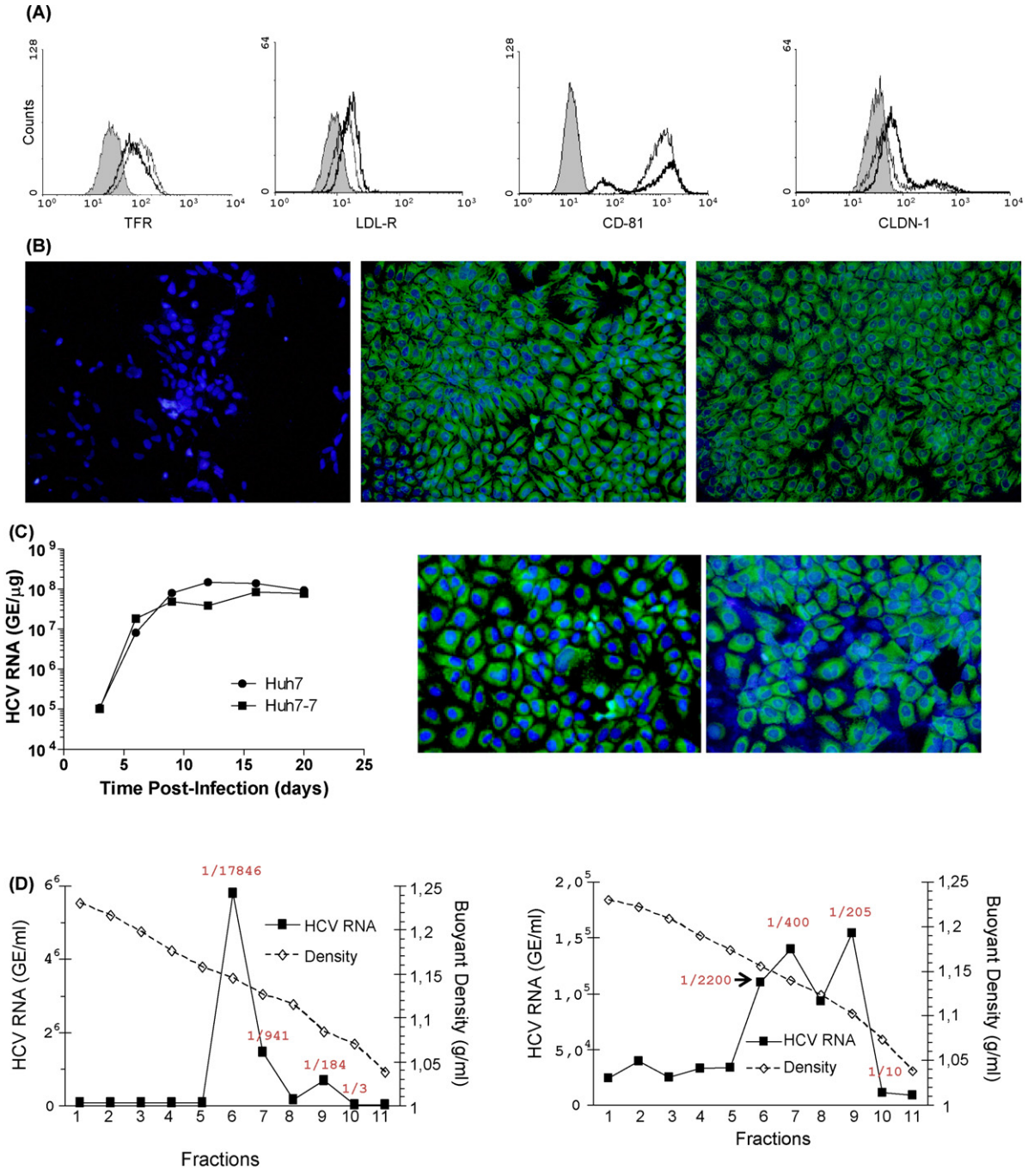

Fig. 1. (A) Cell surface expression of transferrin receptor (TFR), low-density lipoprotein receptor (LDL-R), CD81 and claudin-1 (CLDN-1) on Huh7-7 and Huh7 cells. Isotypic control antibody (filled gray curve), Huh7 cells (thin line), Huh7-7 cells (thick line). (B) Detection of human albumin protein by immunofluorescence in HEK-293, Huh7 and Huh and Huh7-7 cells. (C) (Left) HCV replication following infection with JFH1 virus in Huh7 and Huh7-7 cells. Infected cells were harvested at the indicated time points post-infection. Intracellular RNA was analyzed by qRT-PCR and displayed as genome equivalents (GE)/µg of total RNA. (Right) Immunofluorescence staining of HCV NS5A at 15 days post-infection. (D) Sucrose gradient sedimentation of infectious HCVcc. Supernatant from infected Huh7 (left) and Huh7-7 (right) cells. The specific infectivity (infectious titer/RNA copies) is also indicated for fraction 6, 7, 9 and 10 (in red) (For interpretation of the references to color in this figure legend, the reader is referred to the web version of the article.).

recovered in the supernatant of Huh7 (1/1960) and Huh7-7 (1/1533) cells was comparable. In fact, we and others have proposed that CD81 expression is essential for HCV infection (Labonté et al., 2009; Koutsoudakis et al., 2007). However, it has been clearly shown that CD81-independent infection occurs in a mixed population where the virus can spread from the cells expressing CD81 to those that do not express it (Timpe et al., 2008).

We also analyzed the state of the virus secreted *in vitro* by the Huh7-7 population (Fig. 1D, right). As expected, the most infectious virus was present in the lower density fractions (1.06–1.1 g/ml), whereas the virus present in the highest density fractions (1.13–1.16) was less infectious. Interestingly, even within the peak of low-density virus, the specific infectivity increased significantly in the lightest fractions, suggesting that the quantity of lipids associated with the viral particles is important (Fig. 1D; fraction 9 and 10).

3.2. Viremia in the HCV xenograft mouse model

To initiate viral replication in mice, two different approaches were evaluated. The first method consisted of the intratumoral injection of HCV JFH1 in naïve tumors and the second method was based on the development of tumors using human cells previously infected *in vitro* (Fig. 2B and C). All tumors developed

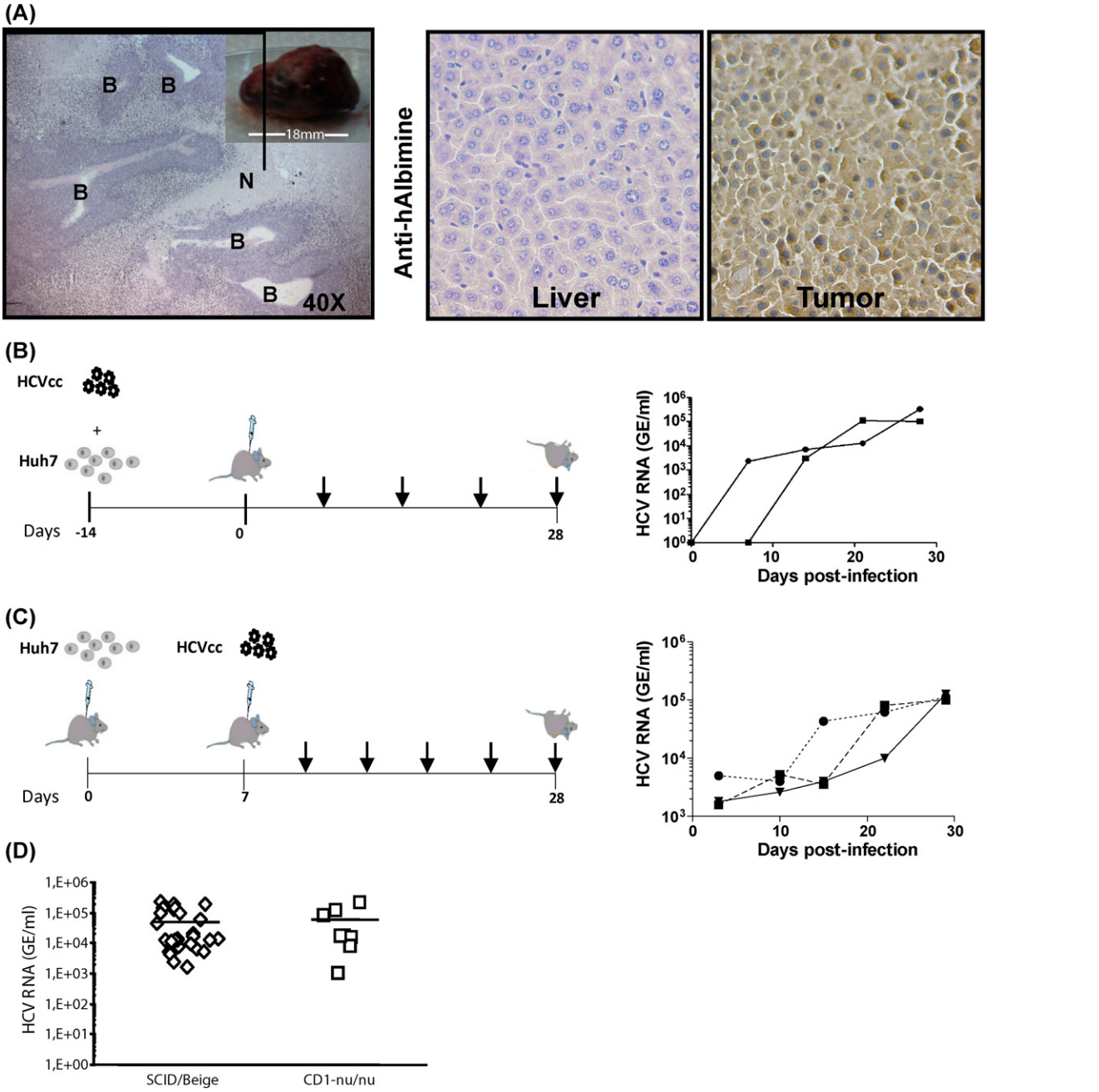

Fig. 2. (A) (Left) Hematoxylin and eosin (H&E) staining of a human hepatocarcinoma xenograft tumor in SCID/beige mice (original magnification 40×). Letter B indicates the presence of blood vessels and letter N indicates necrotic areas in tumor tissues. The upper inset represents a macroscopic view of a human hepatocarcinoma xenograft tumor removed from a SCID/beige mouse. (Right) Immunohistochemical staining of mouse liver tissue and its corresponding human HCC with an anti-human albumin antibody. (B) (Left) Experimental procedure of the HCV-infected xenograft mouse model. Huh7-7 cells infected for 14 days were injected subcutaneously into SCID/beige mice and followed for 4 weeks. (Right) Analysis of the JFH1 RNA viremia in two representative mice. Black arrows show blood sample collection time points. (C) (Left) Experimental procedure of *in vivo* infection of ongoing tumors. (Right) Analysis of the JFH1 RNA viremia in three representative mice. (D) Viremia measured at 4 weeks post-infection in SCID/beige mice (open diamonds, $n = 30$) and CD1 nu/nu mice (open squares, $n = 7$).

Table 2
Relationship between HCV RNA and tumor size.

Tumor size	Tumor (mm^3)	Serum (GE/ml)	Tumor (GE/mg of RNA)	Tumor (GE/mg of tissue)	Total (GE/mouse)
+	726	3.0×10^4	1.7×10^7	1.7×10^7	1.2×10^{10}
++	1800	1.0×10^4	2.6×10^7	1.8×10^7	3.2×10^{10}
+++	3890	3.8×10^5	1.4×10^7	3.9×10^7	1.5×10^{11}

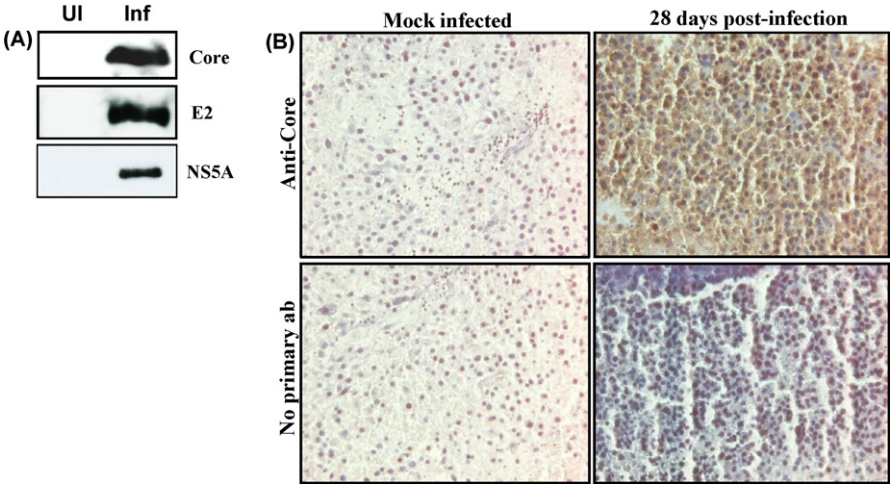

Fig. 3. Immunohistochemistry and expression of HCV JFH1 proteins in tumors isolated 4 weeks post-injection of HCV-infected Huh7 cells. (A) Western blot analysis of viral protein cores, E2 and NS5A, from tumors of uninfected (UI) and infected animals (Inf). (B) Immunohistochemical analysis of tumor tissues from mock-infected or 28-day infected SCID/beige mice using an antibody against the HCV core protein.

using the Huh7-7 cells were extremely vascularized and expressed human albumin (Fig. 2A). HCV titers were determined by measuring the number of copies of positive-strand HCV RNA in mouse sera using quantitative RT-PCR (Taqman). Viremia was analyzed weekly until mice were sacrificed at 4 weeks post-infection. HCV viremia was often detectable as soon as 1 week post-implantation and increased in parallel with tumor size. Furthermore, viremia persisted in animals until sacrifice and the virus titers found in CD1 nu/nu mouse sera were similar to those observed in SCID/beige mice (10^3–10^5 GE/ml) (Fig. 2D). Control mice that were injected with naïve Huh7 showed no detectable HCV RNA titers in their sera (data not shown).

3.3. Viral replication in human hepatocarcinoma xenografts

To investigate the ability of Huh7 tumors to sustain HCV JFH1 replication, animals bearing infected tumors were sacrificed, and tumors were removed and processed for RNA, protein and immunohistochemical analysis. Levels of viral RNA replication were determined by calculating the amount of HCV genome equivalent by quantitative RT-PCR in tumor tissues harvested 4 weeks post-injection. It is noteworthy that the quantity of HCV GE per mg of tissue was shown to be relatively similar in all tumors tested, ranging from 1.7 to 3.9×10^7 HCV GE/mg of tissue (Table 2). Therefore, the amounts of HCV RNA in the tumor were proportional to tumor size. However, the levels of HCV RNA found in mouse sera fluctuated, which suggests that virus secretion from the tumor is not directly proportional to the quantity of infected cells. Finally, both structural and non-structural HCV proteins were easily detected in all tumors by Western blot analysis (Fig. 3A).

To visualize the extent of infection within the tumor at the cellular level, immunohistochemistry analysis using antibodies directed against the HCV core protein was performed. The results clearly indicate that within the tumor, nearly 100% of cells express the HCV core protein (Fig. 3B). As a control, mock-infected tissue did not show any specific coloration. Moreover, the liver of infected mice remained negative for HCV RNA and core proteins as analyzed by qRT-PCR and IHC (data not shown).

3.4. Virus recovered from mice is infectious in vitro

To demonstrate that virus detected in the mouse serum is infectious, sera from three different mice were used to infect naïve Huh7 cells. It has been previously suggested that *in vivo* passage of HCVcc increases the specific infectivity of the virus secreted (Lindenbach et al., 2006). We also observed a significant increase in the specific infectivity of the JFH1 virus recovered from mouse sera (Table 3). Interestingly, JFH1 specific infectivity increased over time elapsed *in vivo*. Taken together, these results indicate that the specific infectivity obtained *in vitro* and *in vivo* are consistent with previous

Table 3
Recovery of cell culture infectivity from HCVcc-infected mice.

Virus preparation	Time *in vivo* (weeks)	Time *in vitro* (weeks)	Infectivity (FFU/ml)	Specific infectivity[b] (infectious virion/RNA)
JFH1[a]	n/a	3	1030	1/1533
Mouse A	1	n/a	90	1/689
Mouse B	1	n/a	60	1/525
Mouse C	2	n/a	720	1/152

n/a, not applicable.
[a] Stock of HCVcc produced in Huh7-7 cells.
[b] Average of two quantification.

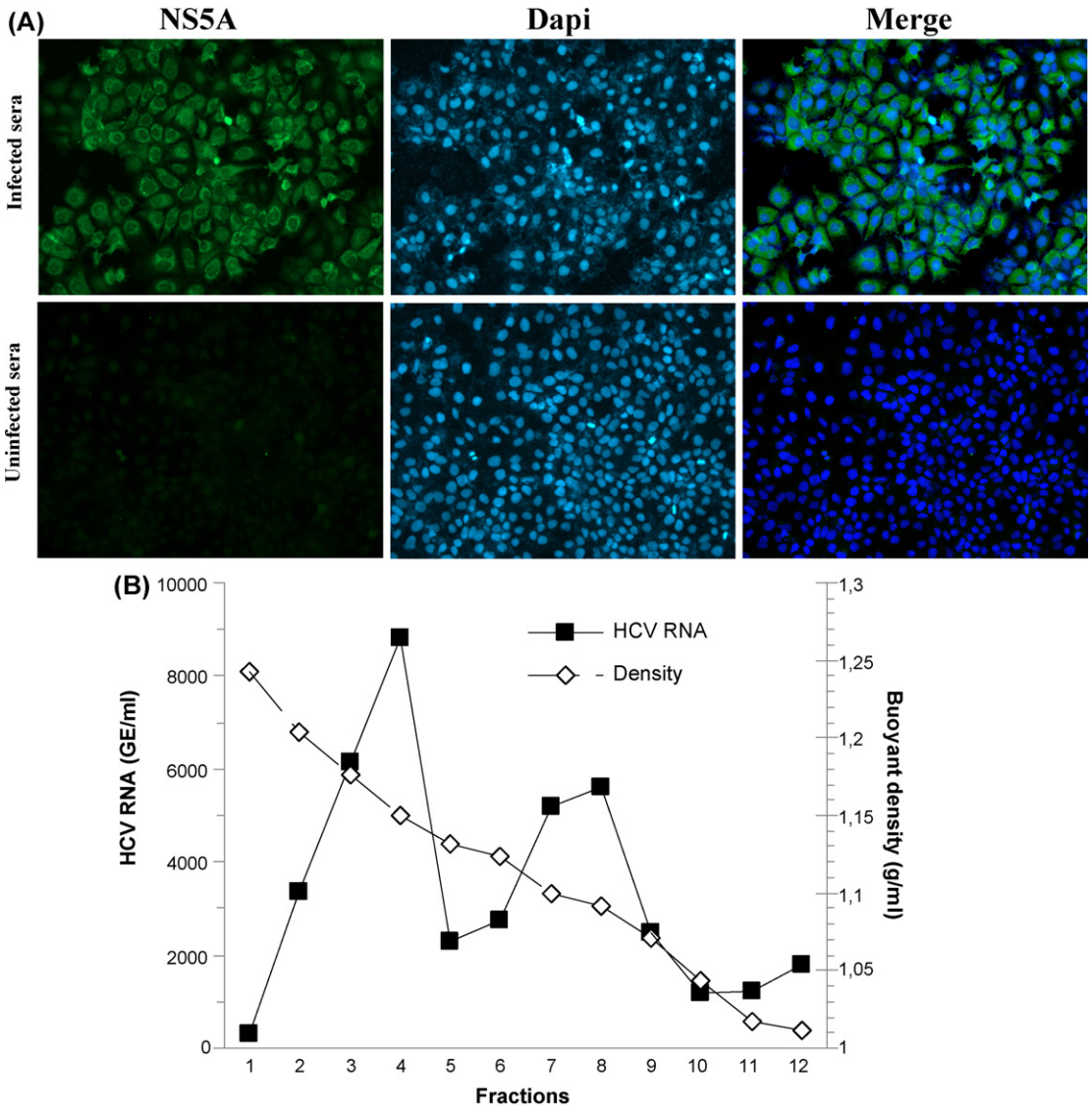

Fig. 4. HCV particles secreted in the mouse sera are infectious *in vitro*. (A) Huh7 cells infected for 15 days with mouse sera were analyzed by immunofluorescence for the presence of the HCV NS5A protein (magnification 100×). (B) Buoyant density of the JFH1 virus from the serum of a mouse at 4 weeks post-infection.

observations and increases during *in vivo* growth (Lindenbach and Rice, 2005; Lindenbach et al., 2006; Wakita et al., 2005; Zhong et al., 2005). Fig. 4A shows a representative set of data demonstrating that HCV JFH1 virus recovered from mouse sera can readily infect and propagate in naïve Huh7 cells *in vitro*. To determine whether the virus secreted in the bloodstream of the mouse segregated into two major peaks, we performed a sucrose gradient centrifugation. Again, the results suggest that the virus is secreted both bound to lipoproteins (1.06–1.1 g/ml) and as unbound virus (1.13–1.16 g/ml) (Fig. 4B).

3.5. Validation of the HCV xenograft mouse model with antiviral agents

To demonstrate the usefulness and the simplicity of this xenograft model, two well-known HCV inhibitors (Intron-A and BILN-2061) were evaluated for their capacity to reduce viremia in infected mice. As anticipated, both inhibitors showed an antiviral effect when administered subcutaneously. Indeed, at 3 or 4 days post-administration of Intron-A or BILN-2061, respectively, all mice showed a decrease in their HCV viremia (Fig. 5A). Furthermore, the viral titer became undetectable in one of the mice treated with Intron-A and with BILN-2061 but this did not occur in the saline group. In fact, the viremia increase in all animals of the saline group produced a >1 log variation over a 5-day treatment period when compared to the IFN-treated mice (Fig. 5B). This result is very similar to recent reports using the SCID-Alb/uPA or HCV replicon mouse model (Kneteman et al., 2006; Zhu et al., 2006). To confirm that the reduction in viremia observed in response to the interferon was due to viral inhibition and not inhibition of tumor growth, we compared the development of the tumor in the presence or absence of Intron-A (Fig. 5C). The results indicated that the administration of Intron-A did not significantly affect tumor development, indicating that the reduction in viremia observed in response to Intron-A was due to its antiviral effect. Interestingly, in our experiment, the NS3 protease inhibitor (BILN-2061) was more potent than interferon, with a clear decrease in viremia over a 4-day treatment period (Fig. 5B). In the case of BILN-2061, all three mice injected with the compound showed normal tumor development when compared with the saline group (data not shown) and no adverse effect was observed upon visual examination.

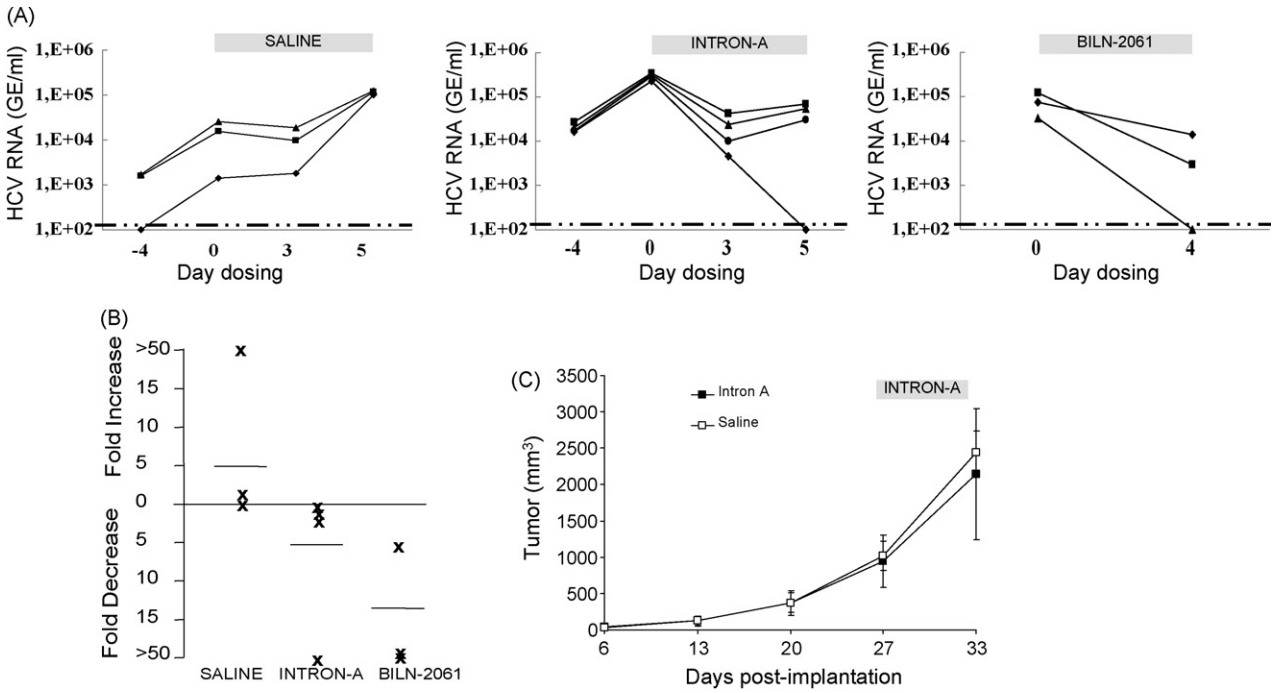

Fig. 5. Effect of HCV inhibitors on HCV replication *in vivo*. (A) Subcutaneous injection of Intron-A and BILN-2061 was initiated when the tumor volume reached 250 mm^3. Intron-A was administered at 20,000 IU/day for 5 days ($n = 4$), BILN-2061 at 30 mg/kg/day for 3 days ($n = 3$) and saline once daily for 5 days ($n = 3$); each bar represents an individual mouse. Dashed lines represent the limit of detection of the qRT-PCR. (B) Fold changes of HCV RNA viremia in mice treated with saline, Intron-A or BILN-2061. Comparison was made between day 0 and day 5 (saline and Intron-A) or day 0 and day 4 (BILN-2061). (C) IFN-α2b treatment did not affect the tumor growth rate. Tumor size in mice treated with 20,000 IU IFN/days for 5 days ($n = 5$) or saline solution ($n = 6$) (error bars show SD).

4. Discussion

In vivo replication of HCV in a simple reproducible system is essential for the evaluation of new classes of antiviral agents. *In vitro*, the replication of HCV or HCVcc is restricted to primary hepatocytes and Huh7 cells, respectively (Fournier et al., 1998; Molina et al., 2007; Wakita et al., 2005). Therefore, strategies have been developed to produce animal models based on both cell types (Ilan et al., 2002; Kneteman et al., 2006; Labonté et al., 2002; Mercer et al., 2001). Here, we report the first simple and convenient mouse model that used a Huh7-derived cell population to produce infectious HCV in mice.

Previous reports indicated that Huh7 cells could be tumorigenic (Chiba et al., 2006; Esposito et al., 2006; Kito et al., 2003). However, in our hands, the engraftment rate of several sources of Huh7 was inconsistent from experiment to experiment (Labonté et al., 2000 and unpublished data). Therefore, the isolation of a stable population of tumorigenic and HCV-permissive Huh7 cells became necessary to facilitate the standardization of the model. For this purpose, small pieces of tumor were serially passaged in mice. The resulting population, named Huh7-7, remained as susceptible to HCV JFH1 infection as the normal Huh7 cells but showed a significant improvement in the engraftment success rate (Table 1).

To simplify the methodology and to normalize the results, we choose to engraft human cells that had been infected *in vitro*. Indeed, this approach resulted in tumors in which almost 100% of cells were infected, and a rapid onset of viremia (Fig. 3B). Therefore, the quantities of HCV RNA found in animals were proportional to the size of the tumors (Table 2). As an alternative, we also infected mice harboring naïve Huh7 tumors by intratumoral injection of HCV JFH1, and observed efficient infection of the animal (Fig. 2C). It is interesting to note that it was possible to detect the virus in the sera of the mice at low buoyant density, indicating the secretion of infectious particles coated with lipoproteins. In this situation, the virus recovered from animals was more infectious than its equivalent obtained *in vitro*, suggesting that the quality of the JFH1 virus improves *in vivo*.

In this study, we used an HCVcc of genotype 2a (strain JFH1). Several chimeric HCVcc strains expressing the structural proteins for all six HCV genotypes have also been developed and could be tested in this animal model as well (Gottwein and Bukh, 2008). Obviously, an infectious full-length genotype 1 HCVcc would be extremely valuable for the screening of antiviral drugs. However, the replication of genotype 1 HCVcc, such as H77S, is weak *in vitro* and needs to be improved prior to the development of a robust model (Yi et al., 2006).

Although the *in vivo* model presented here cannot be used to study HCV pathogenesis or the antiviral immune response, it should provide a drug discovery asset with which to guide the selection of anti-HCV drug candidates. Currently, in the absence of a convenient HCV mouse model, HCV inhibitors are often developed without any efficacy data obtained in animals. Indeed, human trials are realized solely based on efficacy data collected *in vitro* and on safety and pharmacokinetic profiles. The simplicity and the convenience of the model presented here should allow its utilization at an early stage in the profiling of a compound and give a more accurate indication of the ability of a compound to block viral replication and infection in an *in vivo* setting.

Conflict of interest

The authors have no commercial or other association that might pose a conflict of interest.

Acknowledgements

We thank T. Wakita for providing pJFH1 and pJFH1-GDD; J. Bedard for BILN-2061; B. Willems for Intron-A; O. Nicolas and D. Leclerc for the anti-NS5A and anti-core antibodies, respectively; and H. Jacomy for technical assistance. This work was supported by

a grant from the Natural Sciences and Engineering Research Council of Canada (312225) to P.L. and grant MOP-89797 from the Canadian Institutes of Health Research (CIHR) to A.L. P.L. received salary support from the "Fonds de la Recherche en Santé du Québec", C.G. was supported by a doctoral grant from the "Fondation Armand-Frappier" and A.L. holds the Jeanne et J.-Louis Lévesque chair in immunovirology from the J.-Louis Lévesque Foundation.

References

Bartenschlager, R., Frese, M., Pietschmann, T., 2004. Novel insights into hepatitis C virus replication and persistence. In: Maramorosch, K., Shatkin, A.J., Murphy, F.A. (Eds.), Advances in Virus Research. Elsevier Academic Press Inc., San Diego, pp. 71–180.

Bukh, J., 2004. A critical role for the chimpanzee model in the study of hepatitis C. Hepatology 39, 1469–1475.

Chiba, T., Kita, K., Zheng, Y.W., Yokosuka, O., Saisho, H., Iwama, A., Nakauchi, H., Taniguchi, H., 2006. Side population purified from hepatocellular carcinoma cells harbors cancer stem cell-like properties. Hepatology 44, 240–251.

Di Bisceglie, A.M., McHutchison, J., Rice, C.M., 2002. New therapeutic strategies for hepatitis C. Hepatology 35, 224–231.

Esposito, V., Palescandolo, E., Spugnini, E.P., Montesarchio, V., De Luca, A., Cardillo, I., Cortese, G., Baldi, A., Chirianni, A., 2006. Evaluation of antitumoral properties of the protease inhibitor indinavir in a murine model of hepatocarcinoma. Clin. Cancer Res. 12, 2634–2639.

Fournier, C., Sureau, C., Coste, J., Ducos, J., Pageaux, G., Larrey, D., Domergue, J., Maurel, P., 1998. In vitro infection of adult normal human hepatocytes in primary culture by hepatitis C virus. J. Gen. Virol. 79, 2367–2374.

Gottwein, J.M., Bukh, J., 2008. Cutting the gordian knot-development and biological relevance of hepatitis C virus cell culture systems. In: Maramorosch, K., Shatkin, A.J., Murphy, F.A. (Eds.), Advances in Virus Research. Elsevier Academic Press Inc., San Diego, pp. 51–133.

Ilan, E., Arazi, J., Nussbaum, O., Zauberman, A., Eren, R., Lubin, I., Neville, L., Ben-Moshe, O., Kischitzky, A., Litchi, A., Margalit, I., Gopher, J., Mounir, S., Cai, W.Z., Daudi, N., Eid, A., Jurim, O., Czerniak, A., Galun, E., Dagan, S., 2002. The hepatitis C virus (HCV)-Trimera mouse: a model for evaluation of agents against HCV. J. Infect. Dis. 185, 153–161.

Kato, T., Furusaka, A., Miyamoto, M., Date, T., Yasui, K., Hiramoto, J., Nagayama, K., Tanaka, T., Wakita, T., 2001. Sequence analysis of hepatitis C virus isolated from a fulminant hepatitis patient. J. Med. Virol. 64, 334–339.

Kito, M., Matsumoto, K., Wada, N., Sera, K., Futatsugawa, S., Naoe, T., Nozawa, Y., Akao, Y., 2003. Antitumor effect of arsenic trioxide in murine xenograft model. Cancer Sci. 94, 1010–1014.

Kneteman, N.M., Weiner, A.J., O'Connell, J., Collett, M., Gao, T.J., Aukerman, L., Kovelsky, R., Ni, Z.J., Zhu, Q., Hashash, A., Kline, J., Hsi, B., Schiller, D., Douglas, D., Tyrrell, D.L.J., Mercer, D.F., 2006. Anti-HCV therapies in chimeric SCID-Alb/uPA mice parallel outcomes in human clinical application. Hepatology 43, 1346–1353.

Koutsoudakis, G., Hermann, E., Kallis, S., Bartensclager, R., Pietschmann, T., 2007. The level of CD81 cell surface expression is a key determinant for productive entry of hepatitis C virus into host cells. J. Virol. 81, 588–598.

Krieger, N., Lohmann, V., Bartenschlager, R., 2001. Enhancement of hepatitis C virus RNA replication by cell culture-adaptive mutations. J. Virol. 75, 4614–4624.

Labonté, P., Begley, S., Guévin, C., Asselin, M.-C., Nassoury, N., Mayer, G., Prat, A., Seidah, N.G., 2009. PCSK9 impedes HCV infection in vitro and modulates liver CD81 expression. Hepatology 50, 17–24.

Labonté, P., Kadhim, S., Bowlin, T., Mounir, S., 2000. Inhibition of tumor growth with doxorubicin in a new orthotopically implanted human hepatocellular carcinoma model. Hepatol. Res. 18, 72–85.

Labonté, P., Morin, N., Bowlin, T., Mounir, S., 2002. Basal replication of hepatitis C virus in nude mice harboring human tumor. J. Med. Virol. 66, 312–319.

Lindenbach, B.D., Meuleman, P., Ploss, A., Vanwolleghem, T., Syder, A.J., McKeating, J.A., Lanford, R.E., Feinstone, S.M., Major, M.E., Leroux-Roels, G., Rice, C.M., 2006. Cell culture-grown hepatitis C virus is infectious in vivo and can be recultured in vitro. Proc. Natl. Acad. Sci. U.S.A. 103, 3805–3809.

Lindenbach, B.D., Rice, C.M., 2005. Unravelling hepatitis C virus replication from genome to function. Nature 436, 933–938.

Mercer, D.F., Schiller, D.E., Elliott, J.F., Douglas, D.N., Hao, C.H., Rinfret, A., Addison, W.R., Fischer, K.P., Churchill, T.A., Lakey, J.R.T., Tyrrell, D.L.J., Kneteman, N.M., 2001. Hepatitis C virus replication in mice with chimeric human livers. Nat. Med. 7, 927–933.

Molina, S., Castet, V., Fournier-Wirth, C., Pichard-Garcia, L., Avner, R., Harats, D., Roitelman, J., Barbaras, R., Graber, P., Ghersa, P., Smolarsky, M., Funaro, A., Malavasi, F., Larrey, D., Coste, J., Fabre, J.M., Sa-Cunha, A., Maurel, P., 2007. The low-density lipoprotein receptor plays a role in the infection of primary human hepatocytes by hepatitis C virus. J. Hepatol. 46, 411–419.

Sarbah, S.A., Younossi, Z.M., 2000. Hepatitis C: an update on the silent epidemic. J. Clin. Gastroenterol. 30, 125–143.

Shoukry, N.H., Sidney, J., Sette, A., Walker, C.M., 2004. Conserved hierarchy of helper T cell responses in a chimpanzee during primary and secondary hepatitis C virus infections. J. Immunol. 172, 483–492.

Simmonds, P., Bukh, J., Combet, C., Deléage, G., Enomoto, N., Feinstone, S., Halfon, P., Inchauspé, G., Kuiken, C., Maertens, G., Mizokami, M., Murphy, D.G., Okamoto, H., Pawlotsky, J.M., Penin, F., Sablon, E., Shin, I.T., Stuyver, L.J., Thiel, H.J., Viazov, S., Weiner, A.J., Widell, A., 2005. Consensus proposals for a unified system of nomenclature of hepatitis C virus genotypes. Hepatology 42, 962–973.

Thimme, R., Bukh, J., Spangenberg, H.C., Wieland, S., Pemberton, J., Steiger, C., Govindarajan, S., Purcell, R.H., Chisari, F.V., 2002. Viral and immunological determinants of hepatitis C virus clearance, persistence, and disease. Proc. Natl. Acad. Sci. U.S.A. 99, 15661–15668.

Timpe, J.M., Stamataki, Z., Jennings, A., Hu, K., Farquhar, M.J., Harris, H.J., Schwarz, A., Desombere, I., Roels, G.L., Balfe, P., McKeating, J.A., 2008. Hepatitis C virus cell–cell transmission in hepatoma cells in the presence of neutralizing antibodies. Hepatology 47, 17–24.

Wakita, T., Pietschmann, T., Kato, T., Date, T., Miyamoto, M., Zhao, Z.J., Murthy, K., Habermann, A., Kräusslich, H.G., Mizokami, M., Bartenschlager, R., Liang, T.J., 2005. Production of infectious hepatitis C virus in tissue culture from a cloned viral genome. Nat. Med. 11, 791–796.

Yi, M., Villanueva, R.A., Thomas, D.L., Wakita, T., Lemon, S.M., 2006. Production of infectious genotype 1a hepatitis C virus (Hutchinson strain) in cultured human hepatoma cells. Proc. Natl. Acad. Sci. U.S.A. 103, 2310–2315.

Zhong, J., Gastaminza, P., Cheng, G.F., Kapadia, S., Kato, T., Burton, D.R., Wieland, S.F., Uprichard, S.L., Wakita, T., Chisari, F.V., 2005. Robust hepatitis C virus infection in vitro. Proc. Natl. Acad. Sci. U.S.A. 102, 9294–9299.

Zhu, Q., Oei, Y., Mendel, D.B., Garrett, E.N., Patawaran, M.B., Hollenbach, P.W., Aukerman, S.L., Weiner, A.J., 2006. Novel robust hepatitis C virus mouse efficacy model. Antimicrob. Agents Chemother. 50, 3260–3268.